

Electronic Supplementary Information

Soft seed-mediated dimensional control of metal–organic framework nanocrystals through oil-in-water microemulsion

Jaedeok Lee,^{‡a} Suhyeon Park,^{‡a} Seojeong Woo,^a Cheongwon Bae,^a Yuri Jeon,^a Mingyu Gu,^a Jeongeon Kim,^a Yeram Kim,^a Sang Yong Nam,^b Jong Hwa Jung^a and Juyeong Kim^{*a}

^aDepartment of Chemistry and Research Institute of Natural Sciences, Gyeongsang National University, Jinju 52828, South Korea

^bDepartment of Materials Engineering and Convergence Technology, Gyeongsang National University, Jinju 52828, South Korea

[‡]These authors contributed equally to this work.

^{*}Corresponding author: Juyeong Kim, Email: chris@gnu.ac.kr

Materials and Methods

Figures S1–S20

Tables S1–S5

Movies S1–S3

References

Materials and Methods

Section 1. Chemicals

Zinc nitrate hexahydrate (98%, $\text{Zn}(\text{NO}_3)_2 \cdot 6\text{H}_2\text{O}$, Sigma-Aldrich), cobalt nitrate hexahydrate (99.999%, $\text{Co}(\text{NO}_3)_2 \cdot 6\text{H}_2\text{O}$, Alfa Aesar), 2-methylimidazole (99%, $\text{C}_4\text{H}_6\text{N}_2$, Sigma-Aldrich), o-xylene (98%, C_8H_{10} , Samchun), benzene (98%, C_6H_6 , Sigma-Aldrich), toluene (99.7%, C_7H_8 , Daejung), ethylbenzene (99%, C_8H_{10} , Sigma-Aldrich), n-propylbenzene (98%, C_9H_{12} , Sigma-Aldrich), n-butylbenzene (99%, C_8H_{10} , Sigma-Aldrich), hydrochloric acid (35.0–37.0%, HCl, Daejung), nitric acid (60.0–62.0%, HNO_3 , Daejung), methyl alcohol (99.5%, CH_3OH , Daejung), tannic acid (ACS reagent, $\text{C}_7\text{H}_5\text{O}_4$, Sigma-Aldrich), malononitrile (99%, $\text{CH}_2(\text{CN})_2$, Sigma-Aldrich), benzaldehyde (99.5%, $\text{C}_7\text{H}_6\text{O}$, Sigma-Aldrich), dodecane (99.5%, $\text{C}_{12}\text{H}_{26}$, TCI), methyl orange (85%, $\text{C}_{14}\text{H}_{14}\text{N}_3\text{NaO}_3\text{S}$, Sigma-Aldrich) and rhodamine B ($\text{C}_{28}\text{H}_{31}\text{ClN}_2\text{O}_3$, Sigma-Aldrich) were purchased and used without further purification. All glassware was cleaned by aqua regia (a mixture of HCl and HNO_3), thoroughly rinsed with deionised water and dried before use. Deionised water (18.2 $\text{M}\Omega \cdot \text{cm}$ at 25 °C) purified by a Merck Millipore Direct Q3 UV Water Purification System was used for all solution preparation and washing. All reactions were performed at room temperature.

Section 2. Synthesis of ZIF crystals

2.1. ZIF-8 crystals with xylene-based microemulsion in different xylene volume ratios

ZIF-8 crystals were synthesised according to a literature method with modification.¹ An aqueous solution of 24 mM $\text{Zn}(\text{NO}_3)_2 \cdot 6\text{H}_2\text{O}$ (500 μL) was rapidly added to 1.32 M 2-methylimidazole (500 μL) while stirred at 500 rpm, followed by injecting xylene-based microemulsion solution (500 μL) in different xylene ratios. Note that the microemulsion solution was prepared by vigorously mixing a certain volume of xylene with 100 mL of deionised water in advance (0%: 0 μL , 0.01%: 30 μL , 0.10%: 300 μL and 0.33%: 1000 μL). The reaction mixture was stirred for 5 min and left undisturbed for 3 h. ZIF-8 crystals were collected through centrifugation (6000 rpm, 10 min) and redispersed in methyl alcohol.

2.2. ZIF-8 crystals with different oil phases

ZIF-8 nanocrystals with different oil phases (benzene, toluene, ethylbenzene, propylbenzene and butylbenzene) were prepared by the same procedure as Section 2.1. The volume of each oil phase was fixed as 300 μL .

2.3. ZIF-67 crystals with xylene-based microemulsion in different xylene volume ratios

ZIF-67 crystals were synthesised according to a literature method with modification.² An aqueous solution of 0.164 mM $\text{Co}(\text{NO}_3)_2 \cdot 6\text{H}_2\text{O}$ (600 μL) was rapidly added to 0.67 M 2-methylimidazole (4 mL) while stirred at 500 rpm, followed by injecting xylene-based microemulsion solution (460 μL) in different xylene ratios. Note that the microemulsion solution was prepared by vigorously mixing a certain volume of xylene with 100 mL of deionised water in advance (0%: 0 μL , 0.03%: 100 μL and 0.10%: 300 μL). The reaction mixture was stirred at 500 rpm for 5 h. ZIF-67 crystals were collected through centrifugation (6000 rpm, 10 min) and redispersed in methyl alcohol.

2.4. Hollow nanostructure

Hollow nanostructure formation was performed according to a literature method with modification.³ ZIF-67 nanocrystals prepared in Section 2.3 were first encapsulated by ZIF-8 shells as follows. Aqueous solutions of 30 mM 2-methylimidazole (2.5 mL) and 30 mM $\text{Zn}(\text{NO}_3)_2 \cdot 6\text{H}_2\text{O}$ (2.5 mL) were added in sequence to ZIF-67 nanocrystal solution (200 μL). The mixture was left undisturbed for 1 h. The product (ZIF-67@ZIF-8) was collected after twice centrifugations (1000 rpm, 10 min) and redispersed in methyl alcohol (5 mL). Then, the core in ZIF-67@ZIF-8 nanocrystals were etched using tannic acid. An aqueous solution of tannic acid (200 μL) in different concentrations (0.6 mM for 0.03% and 3 mM for 0.1%) was added to ZIF-67@ZIF-8 nanocrystal solution. The mixture was left undisturbed for 10 min. The hollow nanostructure was collected after twice centrifugations (3000 rpm, 10 min) and redispersed in methyl alcohol.

Section 3. Application of ZIF crystals

3.1. Knoevenagel condensation reaction

ZIF-8 crystals were thoroughly dried at 100 °C for 6 h under vacuum. ZIF-8 crystals (0.0158 g) were mixed with benzaldehyde (200 μL), dodecane (200 μL) and toluene (400 μL), followed by ultrasonication for 2 min. The mixture was transferred into 1 mL of toluene with malononitrile (0.25 g) and stirred at 200 rpm. An aliquot (200 μL) was collected at 30 min, 1 h, 2 h, 4 h and 6 h and centrifuged to remove ZIF-8 crystals (10000 rpm, 1 min). The supernatant was measured using an Agilent 7890A gas chromatography (Agilent Technologies). Dodecane was used as an internal standard.

3.2. Dye adsorption

ZIF-8 crystals were thoroughly dried at 100 °C for 6 h under vacuum. ZIF-8 crystals (0.01 g) were mixed with 10 mL of an aqueous solution of methyl orange and rhodamine B (50 mg/L) and sonicated for 2 min, respectively. Each solution was stirred at 500 rpm for 2 h. After dye adsorption, the supernatant was acquired by centrifugation (8000 rpm, 10 min) and measured using a Genesis 10S UV–Vis spectrophotometer.

Section 4. Materials characterisation

A FEI Tecnai 12 transmission electron microscope with a LaB6 emitter at 120 kV and S8000 field-emission scanning electron microscope (Tescan) were used for morphology analysis. A Nano ZS Malvern Zetasizer was used to measure dynamic light scattering (DLS). Powder X-ray diffraction was measured using a D8 Advanced A25 diffractometer (BRUKER). BET surface area was measured using a BELSORP-mini II (MicrotracBEL). Thermogravimetric analysis (TGA) was measured using a TGA Q50 (TA Instruments). A TruSpec Micro (LECO) was used for elemental analysis. Microemulsion density and diameter were estimated using a Sympatec particle size analyser (NANOPHOX). A Nikon optical microscope (ECLIPSE 80i) was used for in situ analysis of microemulsion. For cryogenic transmission electron microscopy, a reaction solution (3 μ L) was sampled on a holey carbon-coated gold grid (Quantifoil R 1/4, 300 Mesh, Gold) that was pre-treated for high hydrophilicity using a PELCO easiGlow™. Sample vitrification was performed using a semi-automated vitrification robot (Vitrobot Mark IV, Thermo Scientific) with 100% humidity at 25 °C. Rapid immersion of the TEM grid into liquid ethane after 4 s blotting effectively vitrified the sample.

Figures

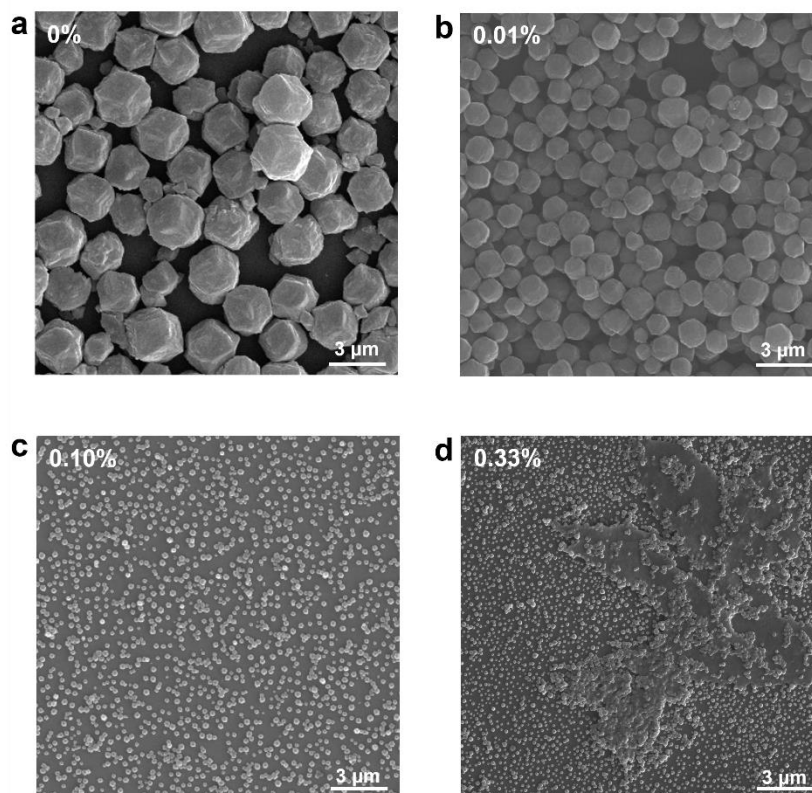


Fig. S1 (a–d) Low-magnification SEM images of ZIF-8 crystals formed by the addition of microemulsion with different xylene volume ratios (a: 0%, b: 0.01%, c: 0.10% and d: 0.33%).

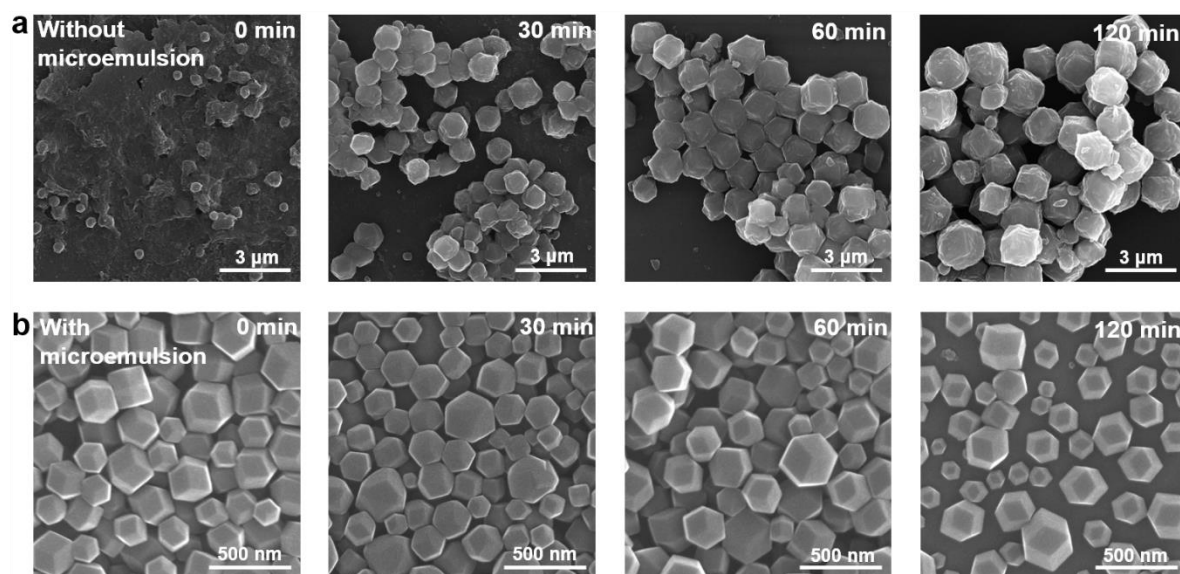


Fig. S2 SEM images of ZIF-8 crystals formed (a) without microemulsion and (b) with microemulsion with 0.10% xylene. At each reaction time, the reaction was terminated and ZIF-8 crystals were collected after removing any remaining chemicals in solution. It is noted that 0 min of reaction was counted right after 5 min of the initial stirring was finished.

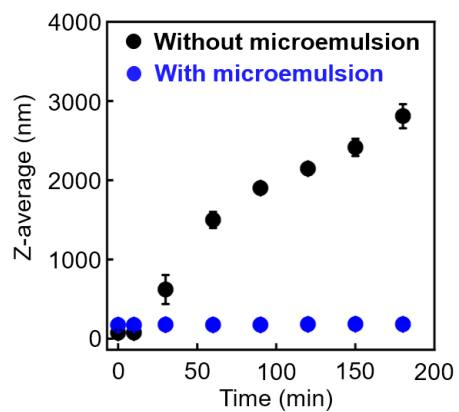


Fig. S3 Size measurement of ZIF-8 crystals as a function of reaction time using DLS (blue circle: ZIF-8 crystals synthesised with 0.10% xylene-based microemulsion and black circle: ZIF-8 crystals synthesised without microemulsion).



Fig. S4 Photographs of as-synthesised ZIF-8 crystal solution with 0.10% xylene-based microemulsion right after the synthesis was terminated. For better visual aid, a scale-up reaction was performed (total volume: 6 mL).

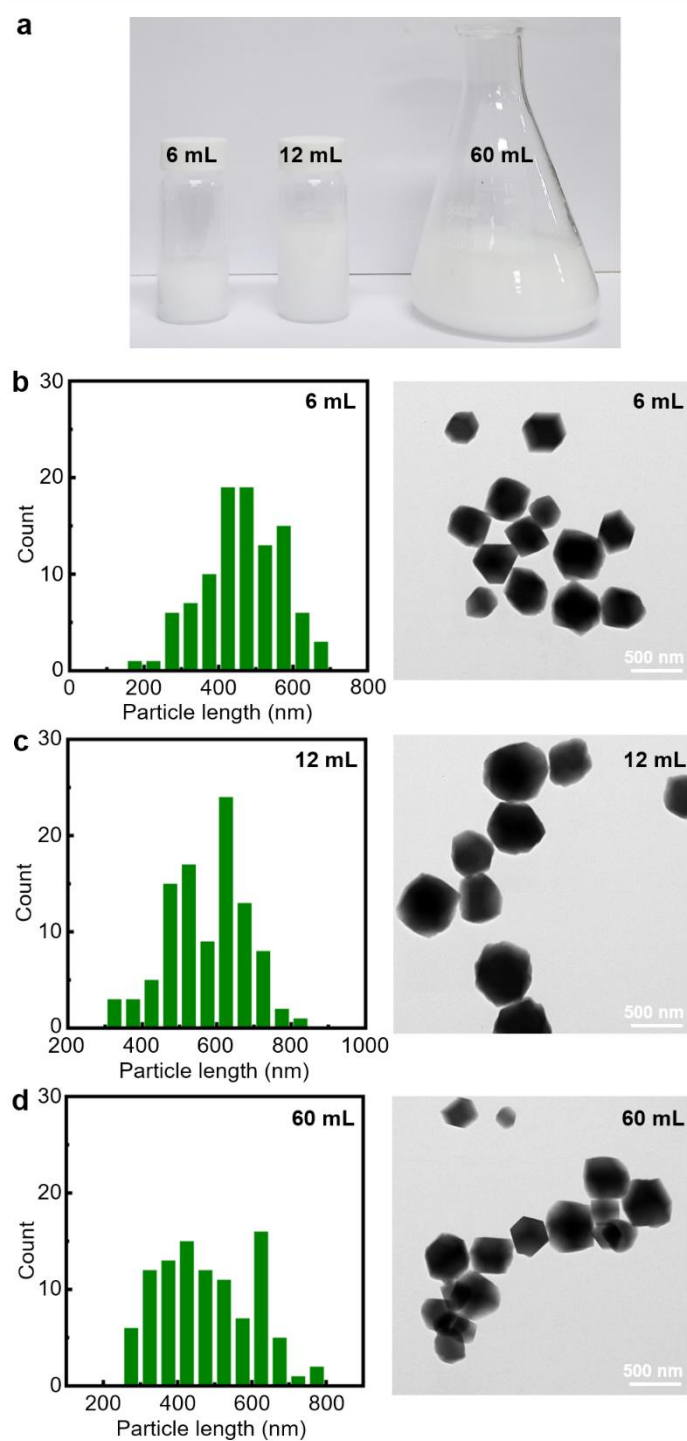


Fig. S5 (a) Photographs of ZIF-8 crystal solution synthesised with 0.10% xylene-based microemulsion (from left to right: 6 mL volume scale, 12 mL volume scale and 60 mL volume scale). Length distribution histogram and representative TEM image of (b) 6 mL volume scale, (c) 12 mL volume scale and (d) 60 mL volume scale. Data were obtained by measuring 100 particles in each condition.

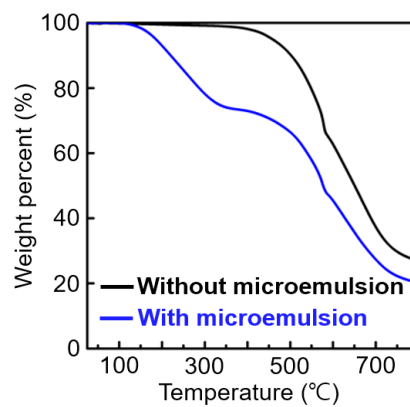


Fig. S6 TGA of ZIF-8 crystals (blue curve: ZIF-8 crystals synthesised with 0.10% xylene-based microemulsion and black circle: ZIF-8 crystals synthesised without microemulsion). The temperature was raised from 25°C to 800°C by 10°C/min under nitrogen.

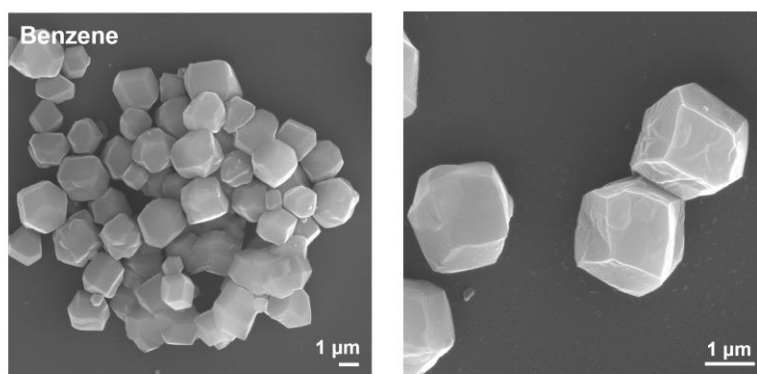


Fig. S7 SEM images of ZIF-8 crystals formed by the addition of 0.10% benzene-based microemulsion.

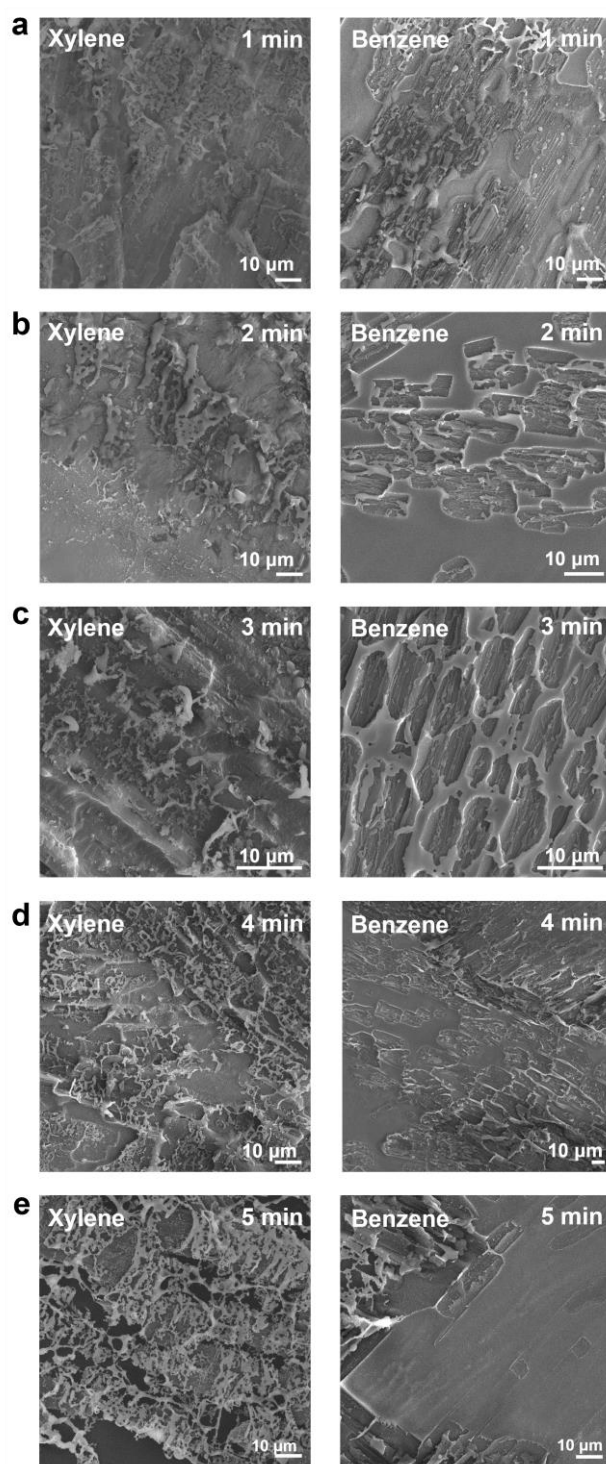


Fig. S8 (a–e) Ex situ SEM images of ZIF-8 crystals captured at different reaction times by 0.10% xylene-based microemulsion (left) and 0.10% benzene-based microemulsion (right).

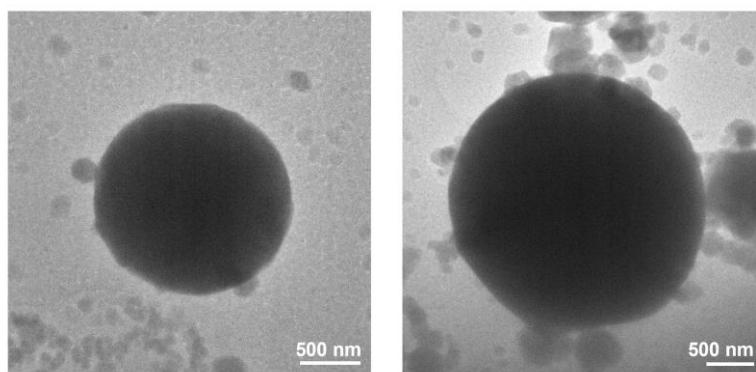


Fig. S9 Cryo-TEM images of a reaction medium frozen at the very early stage of ZIF-8 formation by the addition of 0.10% xylene-based microemulsion.

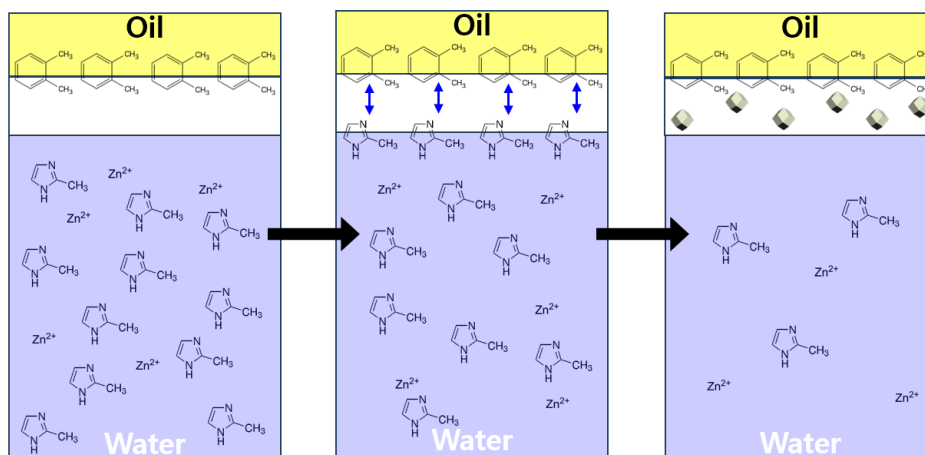


Fig. S10 A schematic for microemulsion-mediated formation of ZIF-8 crystals. At the interface between the microemulsion and bulk solution, the local concentration of 2-methylimidazole could be increased, which accelerated the formation of ZIF-8 crystals.

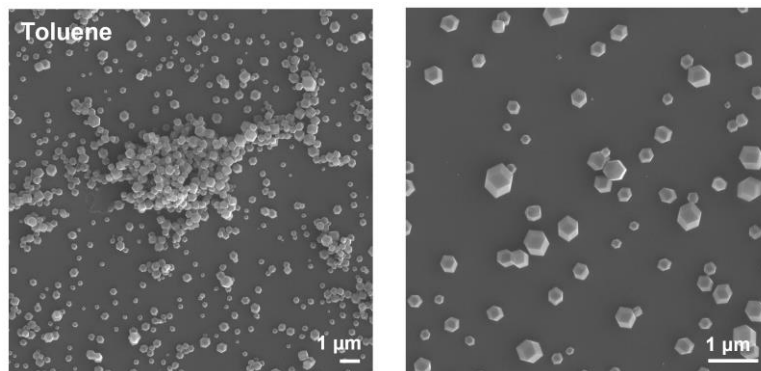


Fig. S11 SEM images of ZIF-8 crystals formed by the addition of 0.10% toluene-based microemulsion.

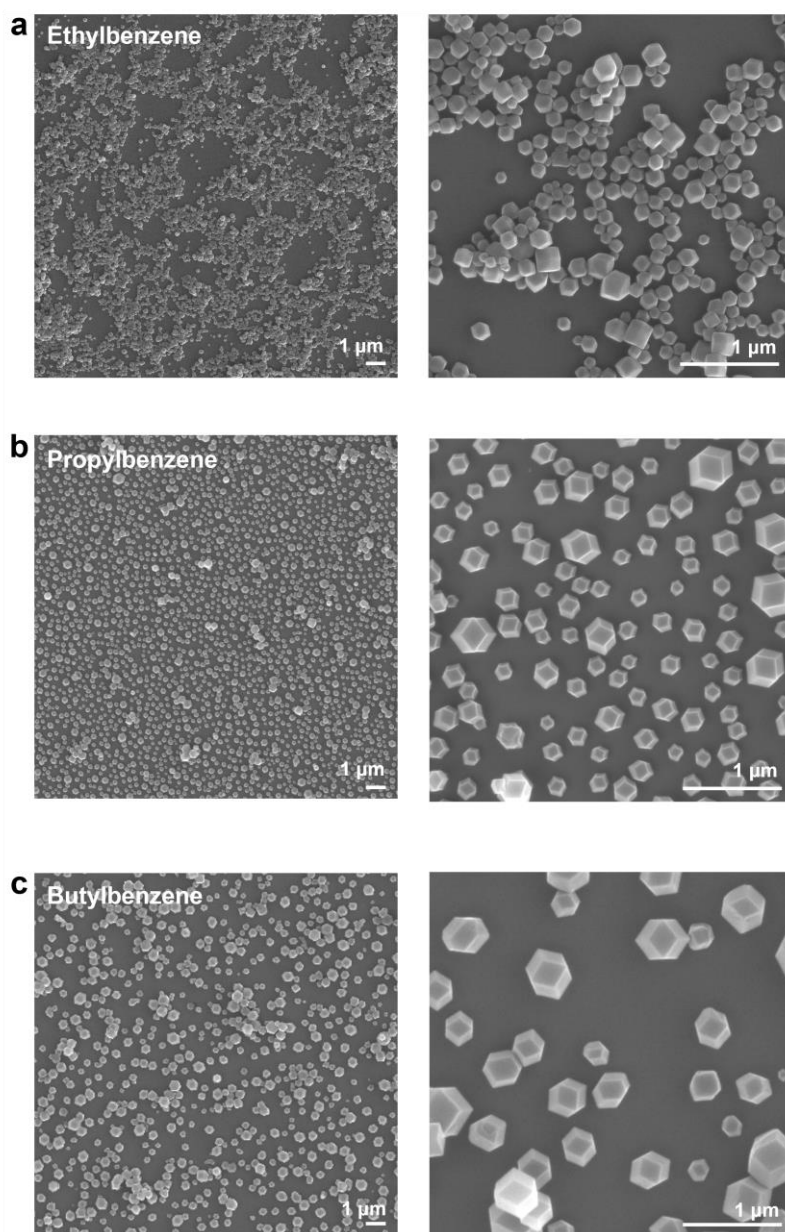


Fig. S12 SEM images of ZIF-8 crystals formed by the addition of (a) 0.10% ethylbenzene-based microemulsion, (b) 0.10% propylbenzene-based microemulsion and (c) 0.10% butylbenzene-based microemulsion.

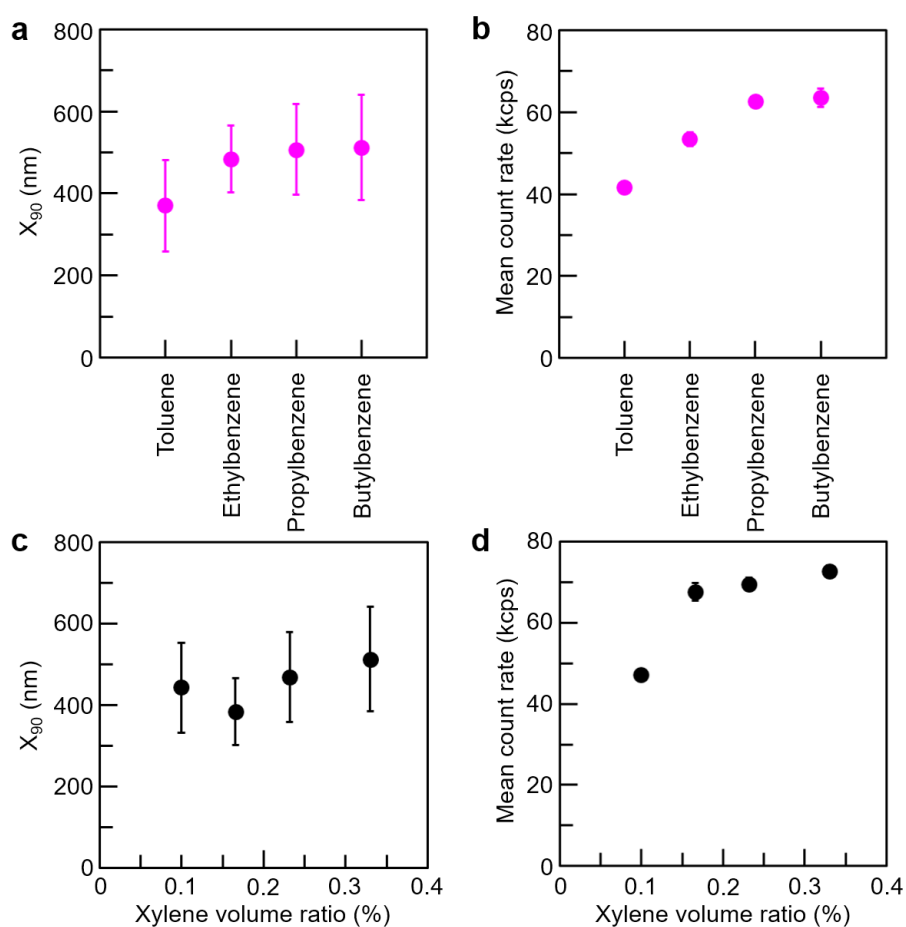


Fig. S13 (a) Oil-in-water microemulsion diameter generated by different oil phases (from left to right: toluene, ethylbenzene, propylbenzene and butylbenzene). (b) Oil-in-water microemulsion density generated by different oil phases (from left to right: toluene, ethylbenzene, propylbenzene and butylbenzene). (c) Oil-in-water microemulsion diameter generated by different xylene volume ratios (from left to right: 0.10%, 0.17%, 0.23% and 0.33%). (d) Oil-in-water microemulsion density generated by different xylene volume ratios (from left to right: 0.10%, 0.17%, 0.23% and 0.33%).

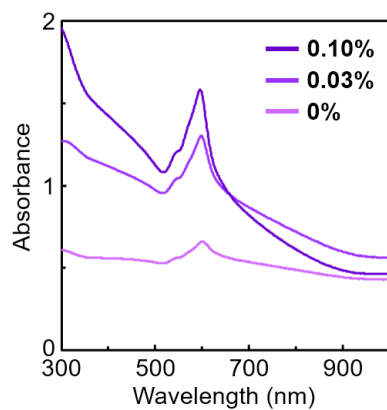


Fig. S14 UV-visible absorption spectra of ZIF-67 crystals formed by the addition of microemulsion with different xylene volume ratios (dark purple: 0.10%, purple: 0.03% and light purple: 0%).

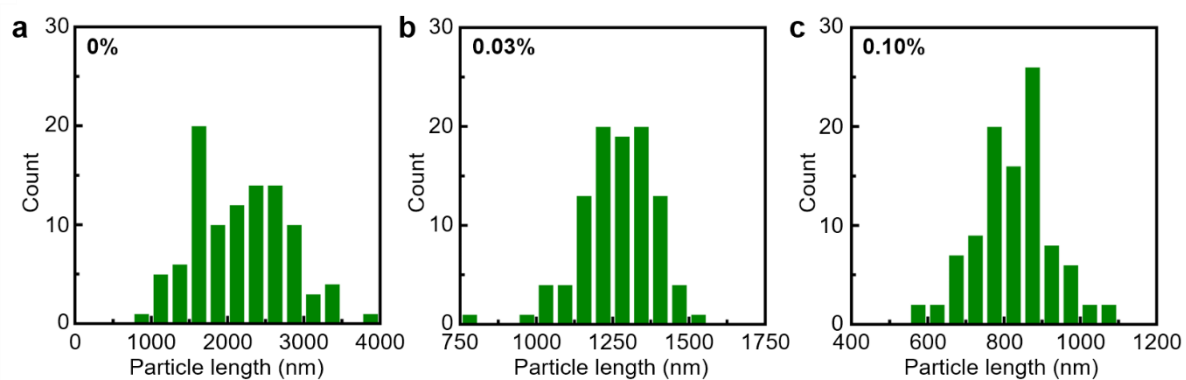


Fig. S15 (a–c) Length distribution histograms for ZIF-67 crystals formed by the addition of microemulsion with different xylene volume ratios (a: 0%, b: 0.03% and c: 0.10%). Data were obtained by measuring 100 particles in each condition.

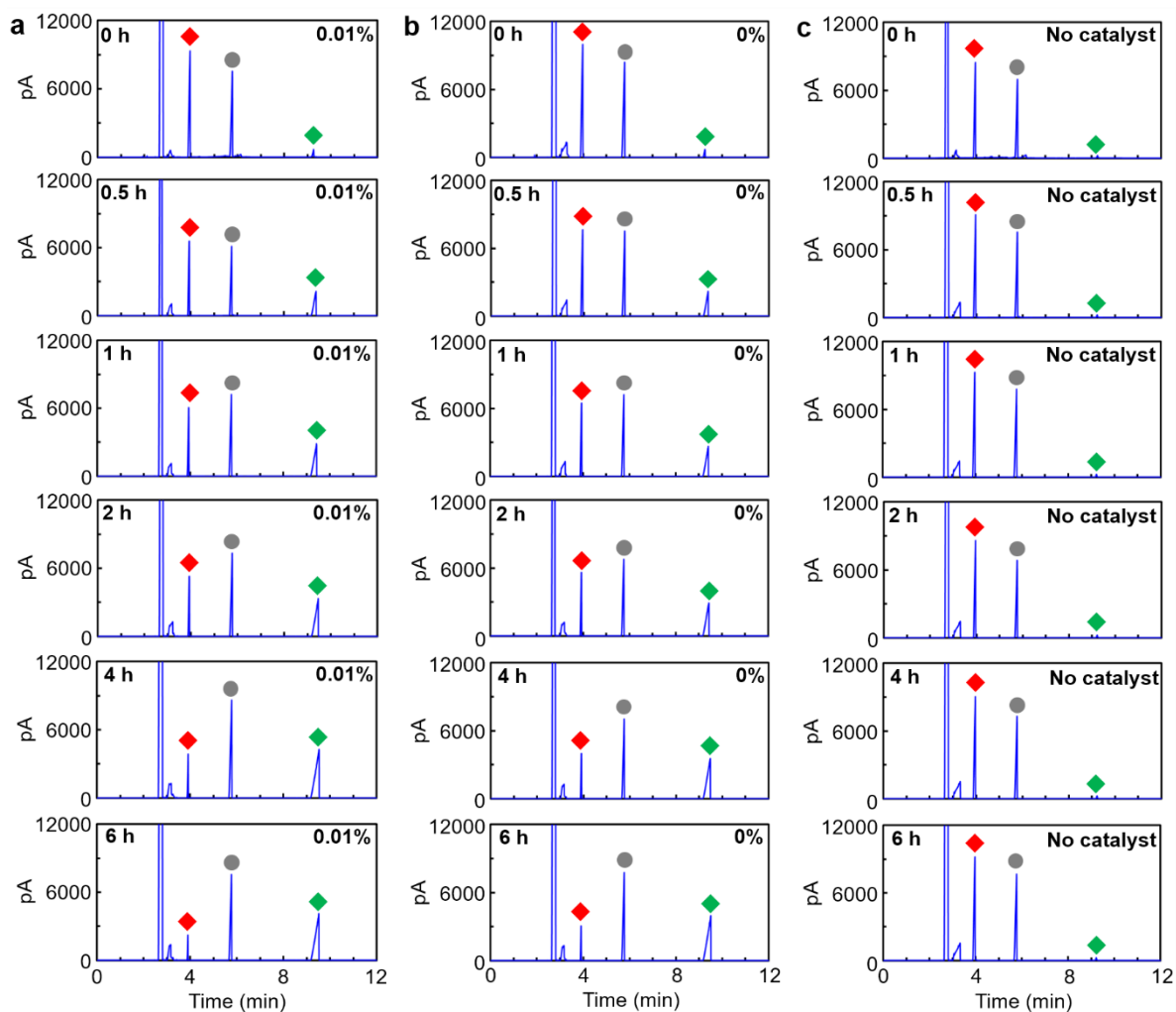


Fig. S16 (a–c) GC spectra of product species collected at different reaction times for Knoevenagel condensation of malononitrile with benzaldehyde using (a) ZIF-8 nanocrystals generated by 0.10% xylene-based microemulsion (a), ZIF-8 microcrystals (b) and no catalyst (c), where peaks were assigned as red rhombus for benzaldehyde, gray circle for dodecane and green rhombus for benzalmalononitrile.

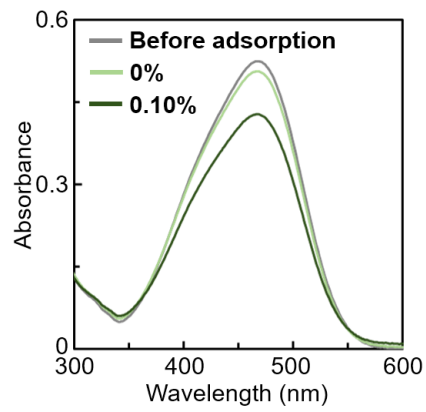


Fig. S17 UV-visible spectra of 50 mg/L methyl orange solution with 0.01 g of ZIF-8 crystals (gray profile: before adding ZIF-8 crystals, light green profile: after adding ZIF-8 microcrystals and dark green profile: ZIF-8 nanocrystals generated by 0.10% xylene-based microemulsion). Each supernatant was measured after diluted 5 times.

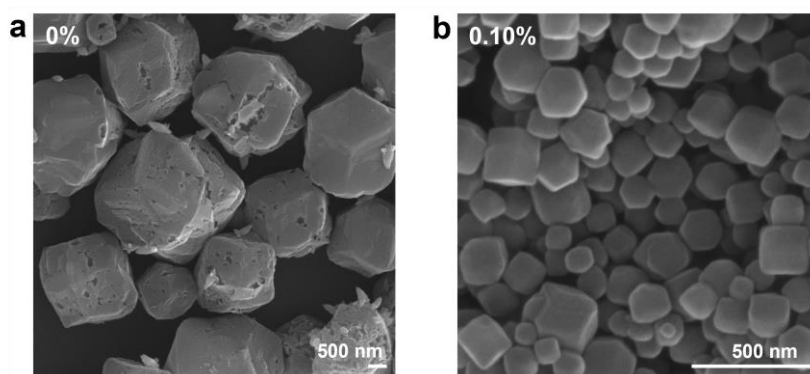


Fig. S18 SEM images of (a) ZIF-8 microcrystals and (b) ZIF-8 nanocrystals generated by 0.10% xylene-based microemulsion after methyl orange adsorption.

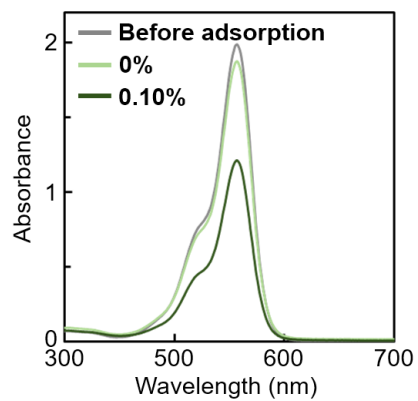


Fig. S19 UV-visible spectra of 50 mg/L rhodamine B solution with 0.01 g of ZIF-8 crystals (gray profile: before adding ZIF-8 crystals, light green profile: after adding ZIF-8 microcrystals and dark green profile: ZIF-8 nanocrystals generated by 0.10% xylene-based microemulsion. Each supernatant was measured after diluted 5 times.

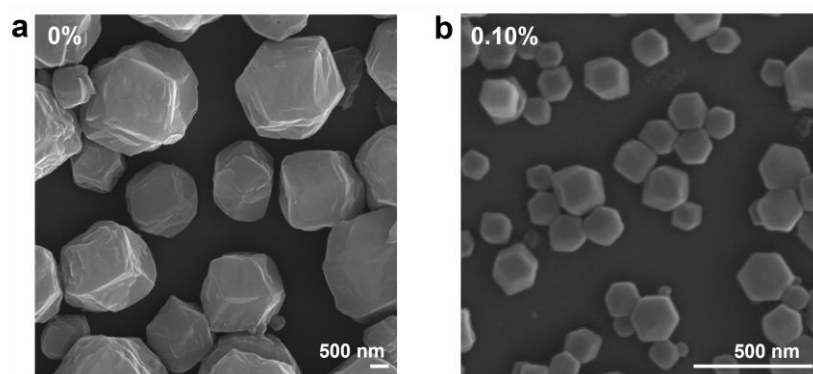


Fig. S20 SEM images of (a) ZIF-8 microcrystals and (b) ZIF-8 nanocrystals generated by 0.10% xylene-based microemulsion after rhodamine B adsorption.

Table S1. Porous structure analysis of ZIF-8 crystals by different volume ratios.

Xylene (%)	BET surface area (m ² /g)	Total pore volume (cm ³ /g)
0	1212	0.6694
0.01	1257	0.6689
0.10	1279	1.2076
0.33	1298	1.1673

Table S2. Elemental analysis of ZIF-8 crystals by different volume ratios.

Xylene (%)	N (%)	C (%)	H (%)
0	25.982	40.189	4.2539
0.10	18.196	54.453	6.6839

Table S3. Conversion rate for the Knoevenagel condensation reaction of malononitrile with benzaldehyde by ZIF-8 in recent work.

Reference	Size (nm)	Conversion (%)
A. L. D. Ramos et al. <i>Appl. Catal. A: Gen.</i> 2017 , 548, 47	21	64 [2 h]
X. Kong et al. <i>Appl. Surf. Sci.</i> 2017 , 423, 349	114	95 [3 h]
D. Bradshaw et al. <i>J. Mater. Chem. A</i> 2018 , 6, 20473	120	77 [6 h]
R. Schneider et al. <i>CrystEngComm</i> 2014 , 16, 4493	141 ± 48	99 [70 min]
L. Rao et al. <i>ChemistrySelect</i> , 2019 , 4, 1188	100–200	88 [10 min]
Our work	272 ± 59	88 [4 h]
W. Ahn et al. <i>Chem. Eng. J.</i> 2015 , 271, 276	300–400	98 [4 h]
X. Kong et al. <i>Appl. Surf. Sci.</i> 2017 , 423, 349	468	65 [3 h]
R. Schneider et al. <i>CrystEngComm</i> 2014 , 16, 4493	500	88 [70 min]

Table S4. Adsorption of methyl orange by ZIF-8 in recent work.

Reference	Size (nm)	Q _e (mg/g)
A. Chiang et al. <i>Microporous Mesoporous Mater.</i> 2019 , 277, 149	50–100	10.1
Our work	272 ± 59	4.8
J. Yao et al. <i>Microporous Mesoporous Mater.</i> 2016 , 234, 287	500	1.8
J. Yao et al. <i>RSC Adv.</i> 2016 , 6, 109608	500	18

Table S5. Adsorption of rhodamine B by ZIF-8 in recent work.

Reference	Size (nm)	Q _e (mg/g)
A. Chiang et al. <i>Microporous Mesoporous Mater.</i> 2019 , 277, 149	50–100	25.0
A. Rehman et al. <i>Surf. Interfaces.</i> 2022 , 34, 102324	< 200	6.9
Our work	272 ± 59	10.0
J. Yao et al. <i>Microporous Mesoporous Mater.</i> 2016 , 234, 287	500	7.8
M. Nath et al. <i>ChemistrySelect</i> 2017 , 2, 7711	> 500	1.6

Movie S1. Real-time recording of 0.10% xylene-induced microemulsion solution under dark.

Movie S2. Real-time recording of 0.10% benzene-induced microemulsion solution under dark.

Movie S3. Real-time recording of xylene-induced microemulsion solution with different volume ratio (from left to right: 0.10%, 0.33%, 1.00% and 3.33%).

References

1. C. Bae, J. Lee, L. Yao, S. Park, Y. Lee, J. Lee, Q. Chen and J. Kim, *Nano Res.* 2021, **14**, 66-73.
2. J. Qian, F. Sun and L. Qin, *Mater. Lett.* 2012, **82**, 220-223.
3. X. Ge, C. Li, Z. Li and L. Yin, *Electrochim. Acta* 2018, **281**, 700-709.